IOP Conference Series: Materials Science and Engineering

Fault Identification for Transformer Axial Winding Displacement Using Nanosecond IFRA and SFRA Experiments

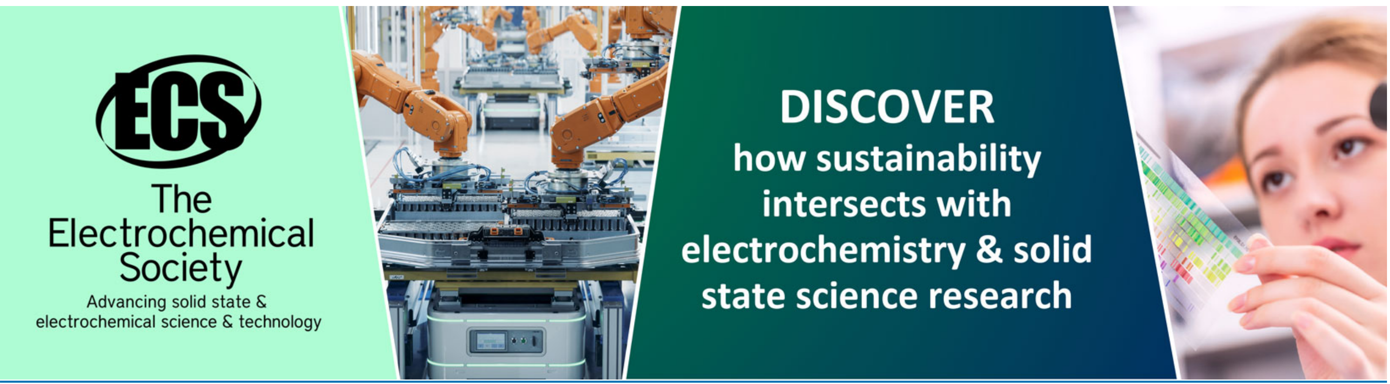

IOP Conf. Series: Materials Science and Engineering **366** (2018) 012067 doi:10.1088/1757-899X/366/1/012067

Fault Identification for Transformer Axial Winding Displacement Using Nanosecond IFRA and SFRA Experiments

J. J. Huang[1], W. H. Tang[1,a], Y. L. Xin[1], J. J. Zhou[1] and Q. H. Wu[1]

[1] School of Electric Power Engineering, South China University of Technology, Guangzhou, 510641, China.

[a]Corresponding author: wenhutang@scut.edu.cn.

Abstract. Nanosecond IFRA has the potential to realize online detection of power transformer winding deformation and displacement. But this method is not mature even in offline condition, and the reliability, accuracy and repeat ability of which are in doubt. To verify the reliability and accuracy of nanosecond IFRA a comparison experiment is conducted between it and a mature method which is applied widely all over the world, SFRA. In this experiment, three levels of axial displacements are experimentally simulated on a dry-type distribution transformer in the lab and both a nanosecond IFRA system and a commercial SFRA analyser are applied to obtain the frequency responses at each fault level separately. To verify the repeatability of Nanosecond IFRA, two Nanosecond IFRA measurements conducted in a time interval of 30 days with all the test condition remaining the same are compared. The results are analysed by visual inspection and quantitative comparison.

1. Introduction

Power transformers are of essential significance, a failure of which may affect the stability and reliability of a power system and its maintenance is costly. According to statistics, a mechanical defect is one of the major causes of power transformer failure. Mechanical defects such as winding deformation and displacement can be caused by short circuit events, transportation and earthquake [1]. These defects may be slight in the beginning, but they are cumulative and may lead to serious incidents in the end. Therefore, it is very important to detect them in its early age and take corresponding measures to diminish the loss.

Frequency response analysis (FRA) is increasingly being used to detect winding mechanical defects [2, 3]. FRA is established upon the fact that the frequency response of a transformer winding depends on its internal distances and profiles [4]. Mechanical defects change the internal distances, thus, cause frequency response variation.

According to the way to obtain winding frequency responses, two kinds of FRA exist, i.e., sweep frequency-response analysis (SFRA) and impulse frequency-response analysis (IFRA). For SFRA, input and output signals are both sinusoidal signals, and a frequency response is obtained dot by dot. For IFRA, input and output are impulse signals which have rich high frequency harmonic components. Usually, Fast Fourier transform (FFT) is employed to transform those impulses into the frequency domain, after that a frequency response is calculated as a whole at one time [5]. SFRA has been applied in industry since 1975, and related standards have been proposed and commercial products have been manufactured [6]. While IFRA has seldom been practiced in comparison with SFRA, it has worse repeatability, lower signal-to-noise ratio and more requirement of measurement equipment [7, 8].

With the development of the digital measurement techniques, the interest in online FRA has increased in recent years. Many researches propose that the transient overvoltage in the electric power system can be used to obtain the frequency response [5]. While other researches state that controlled test signal is more suitable for condition monitoring of transformers. Reference [9] proposed that the test signal can be injected into the transformer in service through the bushing tap. In reference [10], a ferrite transformer was used to isolates the injection circuit from the transformer under test. Reference [11] designed a non-invasive capacitive sensor (NICS) to inject signals into a transformer in service. As recent international standards recommend and many literature suggest the frequency range of FRA test shall be from tens of Hz to 2 MHz [12]. However, reference [13] suggests that the range shall be extended to 10 MHz where the frequency response is more sensible to small changes of winding mechanical defects. In reference [14] by employing NICS for signal injection and acquisition, a Nanosecond IFRA test using an impulse with the width of 400 ns was conducted on a power transformer online and the frequency range was extended to 10 MHz, while the reliability of the results needs verification.

To verify the reliability, accuracy and repeatability of the nanosecond IFRA and to extract the frequency response feature of the axial displacement, this paper conducts an experiment on axial winding displacement within a power transformer by using SFRA and the nanosecond IFRA methods. The results are discussed both by visual inspection and quantitative analysis.

2. Basic principle of FRA

In practice, FRA is usually conducted using the end-to-end measurement connection (EE) [15, 16], as shown in Figure 1 and in this paper, EE is adopted. For SFRA, $V_{in}(t)$ and $V_{out}(t)$ are sweep sinusoidal signals and for IFRA $V_{in}(t)$ and $V_{out}(t)$ are impulse signals, which are transformed into the frequency domain, namely, $V_{in}(f)$ and $V_{out}(f)$ by FFT. An FRA system is connected using coaxial cables, the characteristic impedance of which is 50 Ω and those 50 Ω resistors in Figure 1 are used for impedance matching.

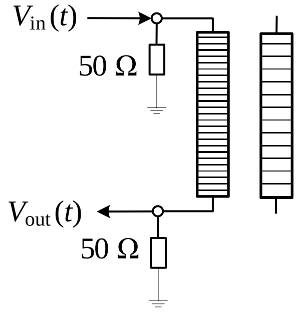

Figure1. End-to-end measurement connection for FRA

The frequency response is determined by the following transfer function:

$$H(f) = 20 \lg \frac{|V_{out}(f)|}{|V_{in}(f)|} \tag{1}$$

FRA compares a frequency response measured at present with one measured at an early stage when the winding is confirmed normal and the difference between them may reveal internal damages of this winding. Above mentioned is so-called time-based (reference) comparison and in many cases due to lack of fingerprints, the construction-based (phase) comparison and type-based (sister unit) comparison are practiced [17].

3. Experiment setup

3.1. Test object

The test object in this research is a dry-type three-phase power transformer (50 kVA, 10/0.4 kV) shown in Figure 2(a). Its high-voltage (HV) winding has 60 discs, and each disc consists of 25 turns of coils. The low-voltage (LV) winding consists of 60 turns of coils. The top 15 discs of the HV winding of each phase is movable and replaceable for experimental purposes, and the rest is fixed. Gaskets can be added between the removable and fixed parts of the winding, as shown in Figure 2(b). A gasket is 10 mm of thickness, and more numbers of gaskets reflects higher severity of axial displacement fault. Three gaskets can be added at most, and the case without any gasket is defined as normal, so, in total, 3 degrees of axial displacement can be experimentally added to the test transformer.

Both the SFRA and IFRA tests are conducted on the same HV winding of the test object in the EE measurement connection with all the other terminal float, and the measurement environment is the same for every test.

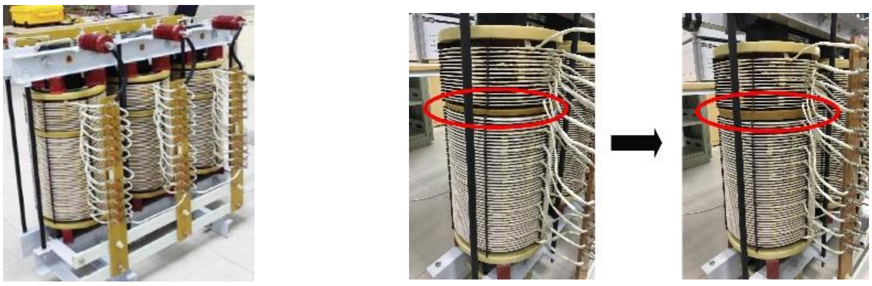

(a) (b)

Figure 2. Test object: (a) Transformer: dry type three-phase power transformer (50 kVA, 10/0.4 kV), (b) Experimental setup for axial displacement

3.2. Test systems

3.2.1. SFRA system The configuration of SFRA test is illustrated in Figure 3. FRAnalyzer has three terminals, that is, a source terminal, a reference terminal and an output terminal. The first two terminals are connected to the input terminal of the test winding. The source terminal injects the sweep sinusoidal signal and the reference records the signal that been injected into the test winding. The output terminal obtains the output signal at the other end of the test winding.

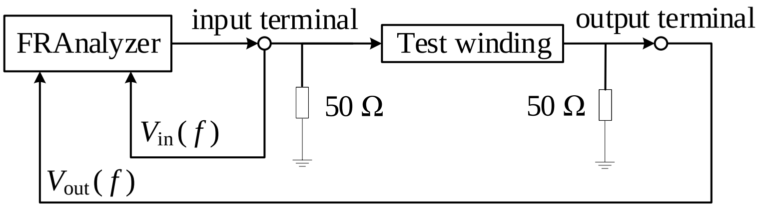

Figure 3. SFRA measurement connection

3.2.2. IFRA system The IFRA system, as shown in Figure 4, is more complicated than the SFRA system. An impulse generator provides a nanosecond double exponential voltage impulse with the rise time of 30 ns and the width of 300 ns and the open circuit peak value is 600 V. This impulse is injected to one terminal of the test winding as the source signal and the reference signal is measured at the same spot by an oscilloscope. The output signal is also measured by the oscilloscope whose sampling frequency is set to 1 GSa/s and the memory length is set to 1 MSa. Since the frequency resolution of frequency response equals the sampling frequency divided by the memory length, the frequency resolution is 1 kHz. The data obtained by the oscilloscope is processed in a computer.

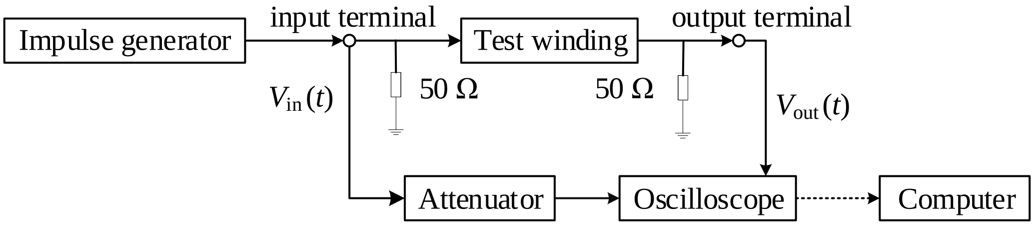

Figure 4. IFRA measurement connection

4. Results and discussion

Figure 5(a) shows a comparison of frequency responses measured by SFRA and IFRA at the same fault level in the same day. The two curves are almost the same to each other, especially in the frequency range under 4 MHz, while there is an obvious difference around 8 MHz. Figure 5(b), (c) show the frequency responses obtained by SFRA and IFRA measured at different fault levels, respectively. They illustrate that the results of SFRA and IFRA have the same trend when the fault degree changes. Two frequency responses obtained by the IFRA system in a time interval of 30 days with other conditions as the same is presented in Figure 5(d). Except the difference around 9 MHz, those two curves are almost the same to each other.

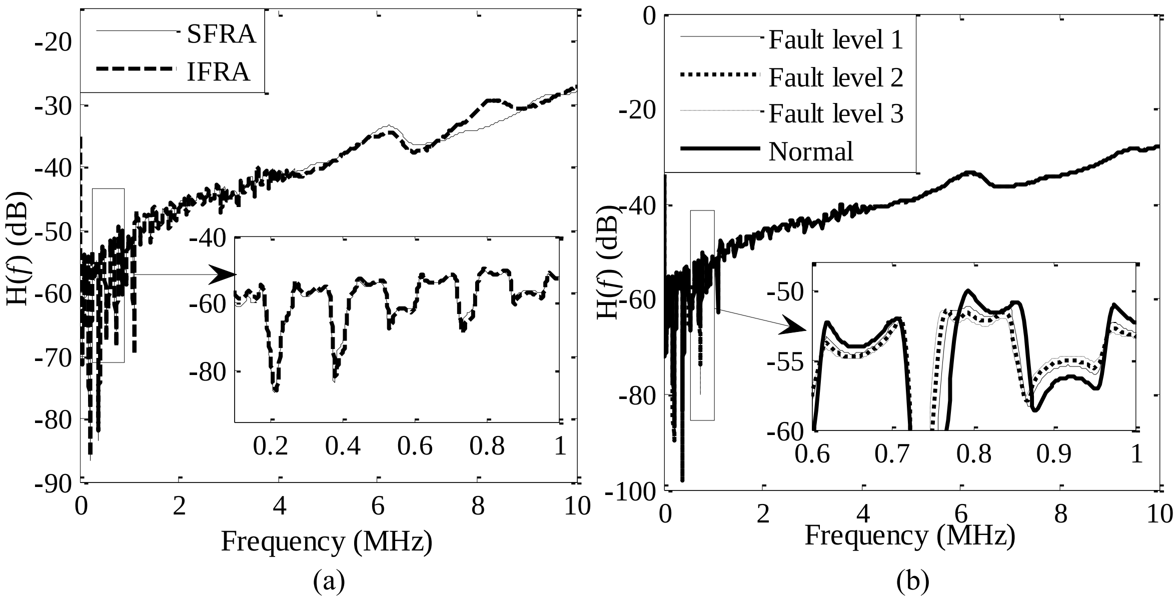

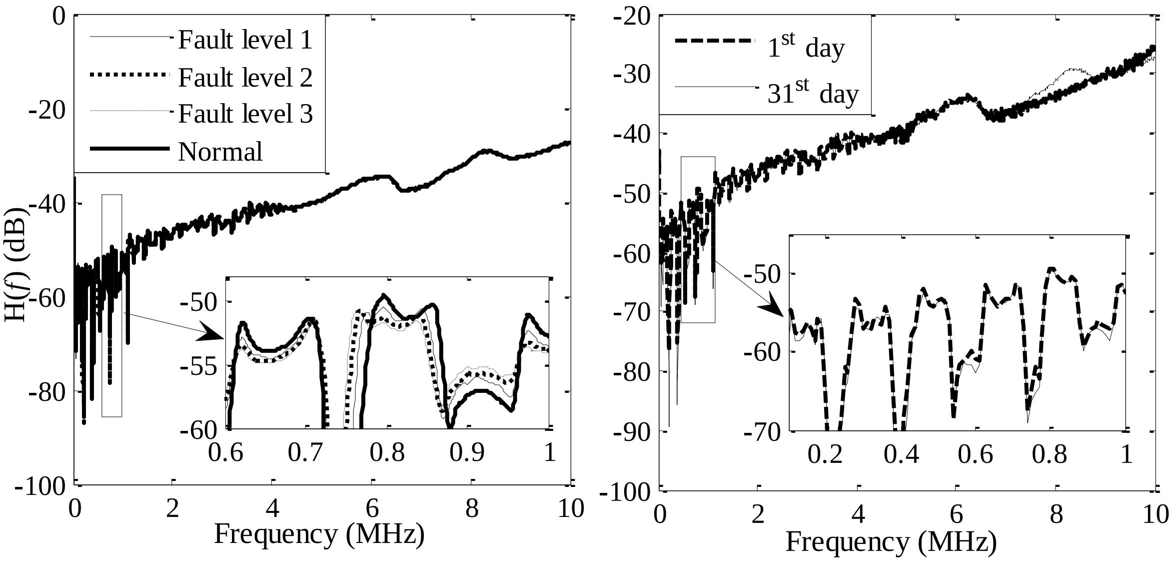

(c) (d)

Figure 5. Frequency responses: (a) Frequency responses obtained by SFRA and IFRA with the same defect degree, (b) Frequency responses obtained by SFRA at different defect degrees, (c) Frequency responses obtained by IFRA at different defect degrees, (d) Frequency responses obtained by IFRA at the same defect degree in a time interval of 30 days.

Apart from the visual inspection, a quantitative analysis can also help assess the severity of mechanical defects. Various statistic indexes can be applied for such purpose [18]. In this paper, the Spearman correlation coefficient, ρ and the Euclidean distance, *ed* are employed. Equations (2) and (3) show how to calculate ρ and *ed* on two frequency responses. x and y are two frequency responses, and each of them contains N points, where based i is the serial number of the points, $\bar{x}$ and $\bar{y}$ are the average of x_i and y_i, respectively. The closer to 1 ρ is or the closer to 0 *ed* is, the more similar to each other x and $y$are. If x is the fingerprint and y is the measured result, higher similarity between them indicates less severity of a fault.

$$\rho = \frac{\sum_{i=1}^{N}(x_i - \bar{x})(y_i - \bar{y})}{\sqrt{\sum_{i=1}^{N}(x_i - \bar{x})^2 \sum_{i=1}^{N}(y_i - \bar{y})^2}} \quad (2)$$

$$ed = \sqrt{\frac{1}{N}\sum_{i=1}^{N}(x_i - y_i)^2} \quad (3)$$

As Figure 5 (a) and (b) shows, in different frequency ranges, the resonance point densities are different, i.e., in the frequency range below 1 MHz, resonance points are closer to each other and the oscillation amplitude of the frequency response is greater, as the frequency becomes higher, the resonance points gradually moves away from each other and the oscillation amplitude decreases. Based on the distribution of resonance point and oscillation amplitude, in this paper, the concerned frequency range is divided into four parts, that is, 1 kHz~1 MHz, 1MHz~2 MHz, 2 MHz~5MHz, 5MHz~10MHz.ρ and *ed* of IFRA results are calculated in each frequency range separately, as presented in Table 1, the minimum value of ρ and the maximum value of *ed* in each row are in bold. The bold numbers only occur in the first column, which shows the axial displacement simulated in this research influences the 1 kHz~1 MHz range the most. And as the severity of the defect increases, ρ decreases and *ed* increases, which is sensible and thus verifies that the results obtained by IFRA are reliable. Table 2 presents ρ of two IFRA frequency response curves measured sequently in a time interval of 30 days, which verified that the nanosecond IFRA has reliable repeatability.

Table 1. Correlation coefficient and Euclidean distance of IFRA frequency responses at different fault levels

index	fault level	1 kHz~1 MHz	1 MHz~2 MHz	2 MHz~5 MHz	5 MHz~10 MHz
ρ	1	**0.9375**	0.9408	0.9925	0.9987
	2	**0.8569**	0.8815	0.9863	0.9985
	3	**0.7959**	0.8351	0.9817	0.9982
ed	1	**2.0063**	0.6518	0.2492	0.1175
	2	**3.0158**	0.9519	0.3383	0.1338
	3	**3.5053**	1.1324	0.3964	0.1361

Table 2. Correlation coefficient of two IFRA frequency response curves in a time interval of 30 days

index	1 kHz~1 MHz	1 MHz~2 MHz	2 MHz~5 MHz	5 MHz~10 MHz
ρ	0.9719	0.9900	0.9661	0.9479

5. Conclusion

This paper has investigated axial winding displacement for a power transformer using SFRA and the nanosecond IFRA experimentally. The visual inspection and quantitative analysis shows that SFRA and the nanosecond IFRA results have great similarity with respect to each other, which proves that the nanosecond IFRA has the same reliability and accuracy as SFRA and its result is repeatable. The experimental also reveals that an axial winding displacement fault mainly effects the 1 kHz~1 MHz frequency range. Moreover, the variation of amplitude of the spectrum is more detectable than the FRA shift of resonance points.

Acknowledgments

This work was supported by National Natural Science of China (No. 51477054).

References

[1] Zhao Z, Yao C, Zhao X, et al. Impact of capacitive coupling circuit on online impulse frequency response of a power transformer. IEEE Transactions on Dielectrics & Electrical Insulation, vol. 23, no. 3, pp. 1285-1293, 2016.
[2] Bengtsson C. Status and trends in transformer monitoring. IEEE Transactions on Power Delivery, vol. 11, no. 3, pp. 1379-1384, 1996.
[3] Leibfried T, Feser K. Monitoring of power transformers using the transfer function method. IEEE Transactions on Power Delivery, vol. 14, no. 4, pp.1333-1341, 1999.
[4] Ryder S A. Diagnosing transformer faults using frequency response analysis. IEEE Electrical Insulation Magazine, vol. 19, no. 2, pp. 16-22, 2003.
[5] Gomez-Luna E, Mayor G A, Gonzalez-Garcia C, et al. Current Status and Future Trends in Frequency-Response Analysis with a Transformer in Service. IEEE Transactions on Power Delivery, vol. 28, no. 2, pp. 1024-1031, 2013.
[6] Dick E P, Erven C C. Transformer Diagnostic Testing by Frequuency Response Analysis. IEEE Transactions on Power Apparatus & Systems, PAS, vol. 97, no. 6, pp. 2144-2153, 2007.
[7] Wang M, Vandermaar A J, Srivastava K D. Review of condition assessment of power transformers in service. IEEE Electrical Insulation Magazine, vol. 18, no. 6, pp. 12-25, 2003.
[8] Liu X, Qiang S. Test research on power transformer winding deformation by FRA method. International Symposium on Electrical Insulating Materials. IEEE, pp. 837-840, 2001.

[9] Rybel T D, Singh A, Vandermaar J A, et al. Apparatus for Online Power Transformer Winding Monitoring Using Bushing Tap Injection. IEEE Transactions on Power Delivery, vol. 24, no. 3, pp.996-1003, 2009.
[10] Gomez-Luna E, Mayor G A, Guerra J P. Application of Wavelet Transform to Obtain the Frequency Response of a Transformer From Transient Signals—Part II: Practical Assessment and Validation. IEEE Transactions on Power Delivery, vol. 29, no. 5, pp. 2231-2238, 2014.
[11] Setayeshmehr A, Akbari A, Borsi H, et al. On-line monitoring and diagnoses of power transformer bushings. Dielectrics & Electrical Insulation IEEE Transactions on, vol. 13, no. 3, pp.608-615, 2006.
[12] BS EN 60076-18:2012, "Power transformers: Part 18 measurement of frequency response," BSI Standards Limited, 2013.
[13] Wang M, Vandermaar A J, Srivastava K D. Improved detection of power transformer winding movement by extending the FRA high frequency range. IEEE Transactions on Power Delivery, vol. 20, no. 3, pp.1930-1938, 2005.
[14] Yao C, Zhao Z, Chen Y, et al. Transformer winding deformation diagnostic system using online high frequency signal injection by capacitive coupling. IEEE Transactions on Dielectrics & Electrical Insulation, vol. 21, no. 4, pp.1486-1492, 2014.
[15] IEEE Standard, "IEEE guide for the application on interpretation of frequency response analysis for oil-immersed transformers," IEEE STd C57.149-2012, Mar.2013
[16] Std. DL/T911-2004, "Frequency response analysis on winding deformation of power transformers," The Electric Power Industry Standard of People's Republic of China, ICS27.100, F24, Document N0.15182-2005, Jun.2005.
[17] Ji T Y, Tang W H, Wu Q H. Detection of power transformer winding deformation and variation of measurement connections using a hybrid winding model. Electric Power Systems Research, vol. 87, no. 87, pp. 39-46, 2012.
[18] Behjat V, Mahvi M, Rahimpour E. New statistical approach to interpret power transformer frequency response analysis: non-parametric statistical methods. Iet Science Measurement & Technology, vol. 10, no. 4, pp.364-369, 2015.